

Optimal harvesting and complex dynamics in a delayed eco-epidemiological model with weak Allee effects

Santanu Biswas · Sourav Kumar Sasmal ·
Sudip Samanta · Md. Saifuddin · Nikhil Pal ·
Joydev Chattopadhyay

Received: 18 June 2016 / Accepted: 6 October 2016 / Published online: 18 October 2016
© Springer Science+Business Media Dordrecht 2016

Abstract In this article, an eco-epidemiological system with weak Allee effect and harvesting in prey population is discussed by a system of delay differential equations. The delay parameter regarding the time lag corresponds to the predator gestation period. Mathematical features such as uniform persistence, permanence, stability, Hopf bifurcation at the interior equilibrium point of the system is analyzed and verified by numerical simulations. Bistability between different equilibrium points is properly discussed. The chaotic behaviors of the system are recognized through bifurcation diagram, Poincare section and maximum Lyapunov exponent. Our simulation results suggest that for increasing the delay parameter, the system undergoes chaotic oscillation via period doubling. We also observe a quasi-periodicity route to chaos and complex

dynamics with respect to Allee parameter; such behavior can be subdued by the strength of the Allee effect and harvesting effort through period-halving bifurcation. To find out the optimal harvesting policy for the time delay model, we consider the profit earned by harvesting of both the prey populations. The effect of Allee and gestation delay on optimal harvesting policy is also discussed.

Keywords Eco-epidemiology · Allee effect · Time delay · Harvesting · Optimal harvesting policy · Saddle node bifurcation · Bistability · Hopf bifurcation · Chaos

1 Introduction

Harvesting of the species and misuse of biological resources are normal in fishery, forestry, agriculture and wildlife management. The pioneering work on this issue was done by Clark [17]. Quite a good number of works were published on harvesting in different systems such as fishery [14], prey–predator models, eco-epidemiological models [5] and time delay models [42]. In ecology, control of disease is one of the major challenges, and the harvesting is a common procedure for controlling the disease. A lot of theoretical studies have been carried out on controlling the disease with culling as a harvesting policy. Harvesting can make a system stable or unstable [18]. Chattopadhyay et al. [13] studied a harvested predator–prey model with

S. Biswas · S. K. Sasmal · S. Samanta · Md. Saifuddin ·
J. Chattopadhyay (✉)
Agricultural and Ecological Research Unit, Indian
Statistical Institute, 203, B. T. Road, Kolkata 700108, India
e-mail: joydev@isical.ac.in

S. Biswas
e-mail: santanubiswas1988@gmail.com

S. K. Sasmal
e-mail: sourav.sasmal@gmail.com

S. Samanta
e-mail: samanta.sudip.09@gmail.com

N. Pal
Department of Mathematics, Visva-Bharati University,
Santiniketan 731235, India
e-mail: nikhilpal.math@gmail.com

infection in the prey population and concluded that harvesting on infected prey prevents the limit cycle oscillations and may be used as a biological control. Harvesting in both the susceptible and infected prey species was studied by Bairagi et al. [5]. They concluded that reasonable harvesting can remove the parasite from their hosts. The authors also concluded that impulsive harvesting can control the cyclic behavior and obtain stable disease-free equilibrium. However, the optimal harvesting policy in such a situation is very important and cannot be ignored as overexploitation can lead to the extinction of the species. For example, due to overexploitation, the *Atlantic cod* population collapsed suddenly in 1992. In another example, the giant bird *Moa* were overexploited to the point of extinction and their predator giant *Haast's eagle* also become extinct. These observations motivate us to study the dynamics under the optimal harvesting policy by using the *Pontryagin's maximum principle*.

Eco-epidemiological models have received much attention from scientists in recent times. The spread of disease among predator–prey interacting populations was first modeled by Haderl and Freedman [25]; after that, Chattopadhyay and Arino [11] coined the term eco-epidemiology for such systems. In recent years, researchers are paying more enthusiasm to consolidate these two critical areas of research, i.e., ecology and epidemiology [4, 12, 28, 62] that have significant biological importance in nature. Biological application of such systems in nature was first demonstrated by Gulland [24]. The main motives of eco-epidemiological models are centered around the role of infection on species mortality, reduction in reproduction rate, characteristics of contamination, change in population size, spread of epidemic waves, permanence of the disease and global behavior of the infected species [51].

Recently, substantial research has been done on the development of the concept for Allee effect, which corresponds to the positive correlation between population size/density and per capita growth rate at low population density [1, 38, 46, 48, 59]. Complications in finding mates, reproductive facilitation, predation, environment conditioning, inbreeding depressions, etc. are few well-known mechanisms behind this Allee effect. Allee effects mainly classified into two ways: strong and weak [20]. Ecologists paid significant attention on this topic as it relates to species extinction [22, 56, 58]. Allee effect and disease are both responsible for extinction of species, and if the disease is combined with the

Allee effects, the interaction between them has substantial biological significance in nature [29, 34, 53–55, 66]. Many species suffer from the Allee effect and the disease. For example, the combined effects of a disease and the Allee effect have been observed in the African wild dogs [19] and the island fox [3]. As a consequence, researchers have paid significant attention on Allee effect in eco-epidemiology [7, 8, 10, 52].

Exploitations in multispecies system are interesting phenomena but not easy to solve both theoretically and practically. On the other hand, time delay may arise in many ecological systems and man-made activities in biology, medicine and other areas (for details see [35] and the references therein). Ignoring time delay means ignoring reality; thus, without delays, dynamical models become a worse conjecture of reality. Various biological reasons lead to the introduction of time delays in models of disease transmission. Time delays used to model the mechanisms in the disease dynamics [30, 44] described a simple HIV/AIDS model with a single class of infective, which incorporates a time delay due to the long incubation period of the disease. Incubation period is the period from the point of infection to the appearance of symptoms of the disease. Time delay plays an important role in biological systems and network of neurons. Propagation time delay (between nodes or in neurons), intrinsic time delay or response time delay that neuron needs to give the response to external forcing. For example, appropriate time delay in autapse of neuron and network can produce complex biological function such as the pacemaker in a network [21, 41, 49, 67]. Kuang [35] concluded that for digesting food, the predator requires some time as time delay. There are numerous research articles on dynamical behaviors such as periodic oscillation, persistence, bifurcation, chaos of population with delayed prey–predator systems [9, 39, 43, 47, 57, 60, 63]. To our knowledge, there are very few works on time delayed population dynamics in the presence of Allee effect [7, 10, 65]. According to the authors, this is the first noble attempt of considering the time delay effects for eco-epidemic models under the influence of Allee effect and harvesting simultaneously in the prey population.

The combined effect of Allee and harvesting in a delayed eco-epidemiology may provide some interesting results. To study the dynamics of such complex system under the optimal harvesting strategy is also another interesting issue. The rest of the article is orga-

nized as follows: Sect. 2 deals with the development of the model. In Sect. 3, we have analyzed the non-delayed model. In Sect. 4, detailed mathematical analysis of our time delayed model has been presented. In this section, we have discussed many important issues such as boundedness of delayed model, uniform persistence, permanence, direction and stability of Hopf bifurcation. The time delayed model shows the chaotic behavior; the existence of chaotic dynamics has been discussed in Sect. 5. In Sect. 6, we have discussed the effect of three important parameters: time lag, inverse of individual searching efficiency and harvesting effort. In Sect. 7, we have discussed the optimal harvesting policy for the time delayed model, to maximize the profit earned by harvesting the prey species (both susceptible and infected) only. The article ends with a discussion.

2 The model

In this section, we develop a delayed eco-epidemiological model with Allee effects and the disease in the prey population.

2.1 General eco-epidemiological model with disease and weak Allee in prey

We start from the assumption that the disease infects the prey population and divides it into two disjoint classes, viz. susceptible (S) and infected (I), so that the total population at any time t is $N = S + I$. Susceptible population is only capable of reproducing, and the infected population dies before having the capacity of reproduction. We also assume that the disease is not vertically transmitted, but it is untreatable and causes an additional death.

We assume that the prey population follows the logistic dynamics with a weak Allee effect in the absence of disease and predation, and can be described by the following single species population model $\frac{dS}{dt} = S(1 - S) \frac{S}{S + \theta}$, where S denotes the normalized healthy prey population. The term $\frac{S}{S + \theta}$ represents the Allee effect function (known as the weak Allee function), which is the probability of finding a mate and θ is the inverse of the individuals searching efficiency [20]. No mating occurs at zero population size, and mating is guaranteed when the population is large (i.e., $\frac{S}{\theta + S} \rightarrow 1$

as $S \rightarrow +\infty$). For small prey population density, bigger values of θ strengthen the Allee effect and slow down the per capita growth rate of the prey.

A general predator–prey model where prey is subjected to the weak Allee effects and the disease is given by the following set of nonlinear differential equations:

$$\begin{aligned} \frac{dS}{dt} &= S(1 - S - I) \frac{S}{S + \theta} - \phi(N) \frac{I}{N} S - g(S, N)P, \\ \frac{dI}{dt} &= \phi(N) \frac{I}{N} S - g(I, N)P - \mu I, \\ \frac{dP}{dt} &= P [cg(S, N) + \gamma g(I, N) - d]. \end{aligned} \tag{1}$$

where all parameters are non-negative: The parameter d represents the natural death rate of predator; the parameter $c \in (0, 1]$ is the conversion rate of susceptible prey biomass into predator biomass; and γ indicates that the effects of the consumption of infected prey on predator. The functions $\phi(N)$ and $g(S/I, N)$ are the general forms of disease transmission function and functional responses, respectively.

2.2 Model with gestation delay

Next, we include two important biological components in the model (1). *First*, after consumption of prey by predator, some amount of energy in the form of prey biomass is converted into predator biomass through a very complicated internal digestion process of the predator. This bio-physiological procedure is not basic; the transformation of prey energy to predator energy is not immediate, and few procedures are included in this complex mechanism. To start with, the portion of prey biomass goes into the digestive system of predator. Digestion is a convoluted process; a few proteins are emitted in the digestive system which act one by one and the prey foods such as starch, protein and fat are processed and changed into monosaccharide, amino acids, fatty acids and glycerol. The digested foods are absorbed in the digestive system of the predator, and the prey food is assimilated into the predator’s protoplasm, i.e., transformed into the predator’s energy in the form of biomass. The whole transformation process requires time; thus, we have considered a constant time lag $\tau (> 0)$ for the gestation of predator [15, 35, 40, 64]. The model becomes

$$\begin{aligned} \frac{dS}{dt} &= S \frac{S}{S + \theta} (1 - S - I) - \phi(N) \frac{I}{N} S - g(S, N)P, \\ \frac{dI}{dt} &= \phi(N) \frac{I}{N} S - g(I, N)P - \mu I, \end{aligned}$$

$$\frac{dP}{dt} = P [cg(S(t - \tau), N(t - \tau)) + \gamma g(I(t - \tau), N(t - \tau)) - d]. \tag{2}$$

2.3 Model with predation only on infected prey

We have neglected the predation on susceptible prey by the predator population and considered that the predator feeds only on infected prey. This assumption supports the experimental evidence provided by Lafferty and Morris [37]. They evaluated that the predation rate on infected fish, on an average, is 31 times higher than the predation rate on susceptible fish. In addition, we have assumed that the consumption of infected prey contributes positive growth to the predator population.

Therefore, a predator-prey model with the above assumptions can be described by the following set of nonlinear differential equations:

$$\begin{aligned} \frac{dS}{dt} &= S \left[(1 - S - I) \frac{S}{S + \theta} - \beta I \right] \\ \frac{dI}{dt} &= I [\beta S - aP - \mu] \\ \frac{dP}{dt} &= \gamma aP(t - \tau)I(t - \tau) - dP \\ &= \alpha P(t - \tau)I(t - \tau) - dP. \end{aligned} \tag{3}$$

For our current study, we have considered disease transmitted through mass action law and predator follows Holling type *I* functional response, where β is the disease transmission rate and a is the predation rate.

2.4 Model with harvesting effort

In this study, we have considered harvesting on the prey populations (both on susceptible and infected prey), while the predator population is excluded from the harvesting process. The lack of economic viability of such harvesting, predator conservation, etc. is various reasons for such exclusions. In effect, both the predator and the harvester are competing for the same resource, namely the prey population. Considering the harvesting effects in (3), we get

$$\begin{aligned} \frac{dS}{dt} &= S \left[(1 - S - I) \frac{S}{S + \theta} - \beta I - q_1 E \right] \\ \frac{dI}{dt} &= I [\beta S - aP - \mu - q_2 E] \\ \frac{dP}{dt} &= \alpha P(t - \tau)I(t - \tau) - dP \end{aligned} \tag{4}$$

where E is the harvesting effort, q_1 and q_2 are the catchability coefficients of the susceptible and infected preys, respectively. All the variables and parameters are positive. The variables and parameters used in the model (4) are presented in Table 1.

The initial conditions for the system (4) take the form

$$\begin{aligned} S(\phi) &= \psi_1(\phi), \quad I(\phi) = \psi_2(\phi), \\ P(\phi) &= \psi_3(\phi), \quad -\tau \leq \phi \leq 0, \end{aligned}$$

where $\psi = (\psi_1, \psi_2, \psi_3)^T \in C_+$ such that $\psi_i(\phi) \geq 0$ ($i = 1, 2, 3$), $\forall \phi \in [-\tau, 0]$, and C_+ denotes the Banach space $C_+([-\tau, 0], \mathbb{R}_+^3)$ of continuous functions mapping the interval $[-\tau, 0]$ into \mathbb{R}_+^3 and denotes the norm of an element ψ in C_+ by

$$\|\psi\| = \sup_{-\tau \leq \phi \leq 0} \{ |\psi_1(\phi)|, |\psi_2(\phi)|, |\psi_3(\phi)| \}.$$

For biological feasibility, we further assume that $\psi_i(0) > 0$, for $i = 1, 2, 3$.

3 Mathematical analysis of the system (4) with no time lag ($\tau = 0$)

In this section, we have analyzed our model without the time delay effect. The system (4) without time delay can be written as

$$\begin{aligned} \frac{dS}{dt} &= S \left[(1 - S - I) \frac{S}{S + \theta} - \beta I - q_1 E \right], \\ \frac{dI}{dt} &= I [\beta S - aP - \mu - q_2 E], \\ \frac{dP}{dt} &= P [\alpha I - d]. \end{aligned} \tag{5}$$

The system (5) has the following boundary equilibria:

$$\begin{aligned} E^0 &= (0, 0, 0), \quad E_i^1 = (S_i, 0, 0), \\ E^2 &= \left(\frac{\mu + q_2 E}{\beta}, \frac{\left(\frac{\mu + q_2 E}{\beta} \right) \left(1 - \frac{\mu + q_2 E}{\beta} \right) - q_1 E \frac{\mu + q_2 E}{\beta} - q_1 E \theta}{\frac{\mu + q_2 E}{\beta} + \beta \theta + \mu + q_2 E}, 0 \right) = (S_2, I_2, 0). \end{aligned}$$

Table 1 Variables and parameters used in the model (4)

Variables/parameters	Biological meaning	Default values
S	Density of susceptible prey	–
I	Density of infected prey	–
P	Density of predator	–
θ	Inverse of the individuals searching efficiency	0.1
β	Rate of infection	0.395
a	Attack rate of predator	0.1
μ	Death rate of infected prey	0.001
α	The total effect to predator by consuming infected prey	0.85
d	Natural death rate of predator	0.1
E	Harvesting effort	0.01
q_1	Catchability coefficients of the susceptible prey species	1
q_2	Catchability coefficients of the infected prey species	1
τ	Gestation time period of predator	–

where S_i are the roots of

$$S_i^2 + S_i(q_1E - 1) + q_1E\theta = 0.$$

$$S_i \text{ exists, if } 1 > q_1E \text{ and } S_1 = \frac{(1-q_1E) + \sqrt{(1-q_1E)^2 - 4q_1E\theta}}{2},$$

$$S_2 = \frac{(1-q_1E) - \sqrt{(1-q_1E)^2 - 4q_1E\theta}}{2}.$$

The system (5) has two interior equilibria $E_1^* = (S_1^*, I_1^*, P_1^*)$ and $E_2^* = (S_2^*, I_2^*, P_2^*)$, where $I_2^* = \frac{d}{\alpha} = I_1^*$, $P_1^* = \frac{1}{a}(\beta S_1^* - \mu - q_2E)$, $P_2^* = \frac{1}{a}(\beta S_2^* - \mu - q_2E)$ and S_1^*, S_2^* are the roots of the quadratic equation

$$(S^*)^2 + S^* \left((\beta + 1) \frac{d}{\alpha} + q_1E - 1 \right) + \left(\beta\theta \frac{d}{\alpha} + q_1E\theta \right) = 0.$$

The interior equilibria exist if $1 - (\beta + 1) \frac{d}{\alpha} - q_1E > 0$ and both of the solutions satisfy $S_1^* > \frac{\mu + q_2E}{\beta}$, $S_2^* > \frac{\mu + q_2E}{\beta}$. Now,

$$S_1^* = \frac{B_{11} - \sqrt{B_{11}^2 - 4C_{11}}}{2} \quad \text{and} \quad S_2^* = \frac{B_{11} + \sqrt{B_{11}^2 - 4C_{11}}}{2}, \tag{6}$$

where $B_{11} = (1 - (\beta + 1) \frac{d}{\alpha} - q_1E)$ and $C_{11} = (\beta\theta \frac{d}{\alpha} + q_1E\theta)$.

Proposition 1 (Local stability of equilibria for the model (5)) *The local stability of equilibria for the Model (5) is summarized in Table 2.*

Proof We have not given the detailed proof in this manuscript (our analysis is similar to the analysis given in [10]). \square

For the set of parameter values in Table 1, we obtain the interior equilibrium point $E_1^* = (0.0056, 0.1176, 0.0121)$ which is an unstable equilibrium and $E_2^* = (0.8303, 0.1176, 3.2696)$ is a stable focus as we see that all the trajectories initiating inside the region of attraction approach toward the equilibrium point $E_2^* = (0.8303, 0.1176, 3.2696)$ (see Fig. 1). Different initial values are chosen as [0.3, 0.1, 0.2], [0.25, 0.2, 0.7], [0.22, 0.40, 1], [0.75, 0.05, 1.2] and [0.1, 0.60, 2] and draw the phase portrait of the system (4) in Fig. 1.

3.1 Saddle node bifurcation

Both S_1 and S_2 exist if $(1 - q_1E)^2 - 4q_1E\theta > 0$. For $(1 - q_1E)^2 - 4q_1E\theta < 0$, E_1^1 and E_2^1 vanishes. So, we can say that depending on the values of E and θ both of these equilibria exist. For

$$\frac{\left(\frac{1}{\sqrt{(q_1E)}} - \sqrt{(q_1E)} \right)^2}{4} = \theta,$$

we observe saddle node bifurcation for the equilibria E_1^1 and E_2^1 .

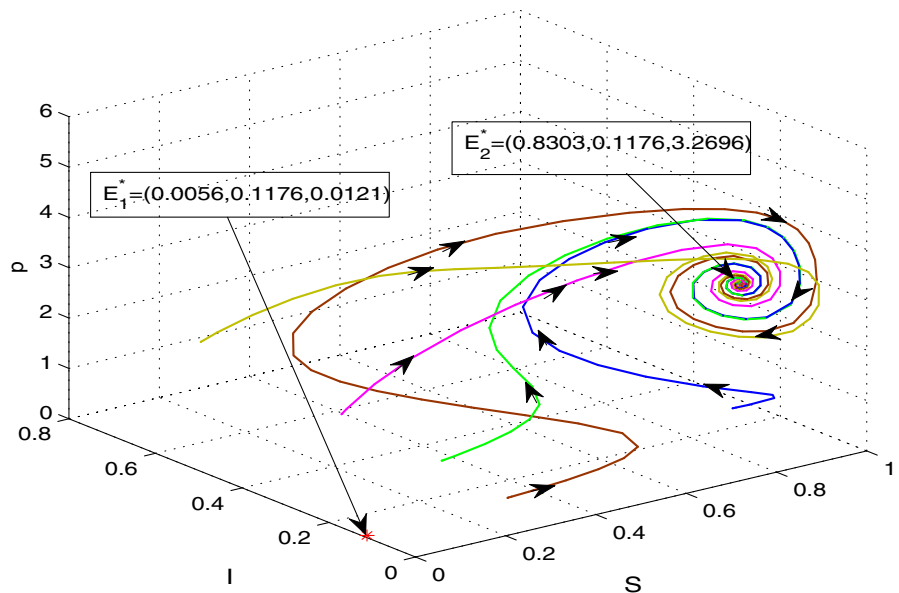
Similarly, saddle node bifurcation between two interior equilibria E_1^* and E_2^* exists for

Table 2 Local stability of equilibria for the model (5)

Equilibria	Existence condition	Stability condition
E^0	Always exists	Always LAS
E_i^1	$1 > q_1 E$ and $(1 - q_1 E)^2 > 4q_1 E\theta$	LAS if $\beta S_i < \mu + q_2 E$ and $q_1 E + \frac{S_i^2}{S_i + \theta} > (1 - S_i)(1 - \frac{\theta^2}{(S_i + \theta)^2})$
E^2	$\frac{\mu + q_2 E}{\beta} \left(1 - \frac{\mu + q_2 E}{\beta}\right) > q_1 E \frac{\mu + q_2 E}{\beta} + q_1 E\theta$	LAS if $-\frac{S_2^2}{S_2 + \theta} - \beta I_2 + \frac{(1 - S_2 - I_2)S_2(S_2 + 2\theta)}{(S_2 + \theta)^2} < q_1 E$ & $\alpha \frac{\left(\frac{\mu + q_2 E}{\beta}\right)\left(1 - \frac{\mu + q_2 E}{\beta}\right) - q_1 E\left(\theta + \frac{\mu + q_2 E}{\beta}\right)}{\frac{\mu + q_2 E}{\beta} + \beta\theta + \mu + q_2 E} < d$
E_2^*	$S_2^* > \frac{\mu + q_2 E}{\beta}$ and $\left(1 - (\beta + 1)\frac{d}{\alpha} - q_1 E\right) > 0$ and $B_{11}^2 > 4C_{11}$	Always LAS when it exists
E_1^*	$S_1^* > \frac{\mu + q_2 E}{\beta}$ and $\left(1 - (\beta + 1)\frac{d}{\alpha} - q_1 E\right) > 0$ and $B_{11}^2 > 4C_{11}$	Unstable

LAS locally asymptotically stable

Fig. 1 Stability of the interior equilibrium for the non-delayed model (5), with default parameter values as in Table 1, with different initial conditions



$$\frac{(1 - (\beta + 1)\frac{d}{\alpha} - q_1 E)}{(\beta\frac{d}{\alpha} + q_1 E)} = \theta.$$

3.2 Bistability

In this subsection, we investigate the possibility of multistability of our model system. We see that the model may be bistable with or without the interior equilib-

rium. Bistability is a phenomenon where the system converges to two different equilibria for the same parametric region based on the variation of the initial conditions. Here we observe that the system (5) shows three types of bistability (see Fig. 2): one is in the presence of interior equilibrium, and the other two are in the absence of interior equilibrium. Any trajectory starting from the interior of \mathbb{R}_+^3 either converges to E^2 , E_1^* or E^0 when interior equilibrium does not exist (depend-

Fig. 2 Bistability region of the system (5). The magenta region shows the bistability of E^0 and E_2^* , the yellow region shows the bistability of E^0 and E^2 , and the red region indicates the bistability of E^0 and E_1^1 . In the white region, only E^0 is stable. (Color figure online)

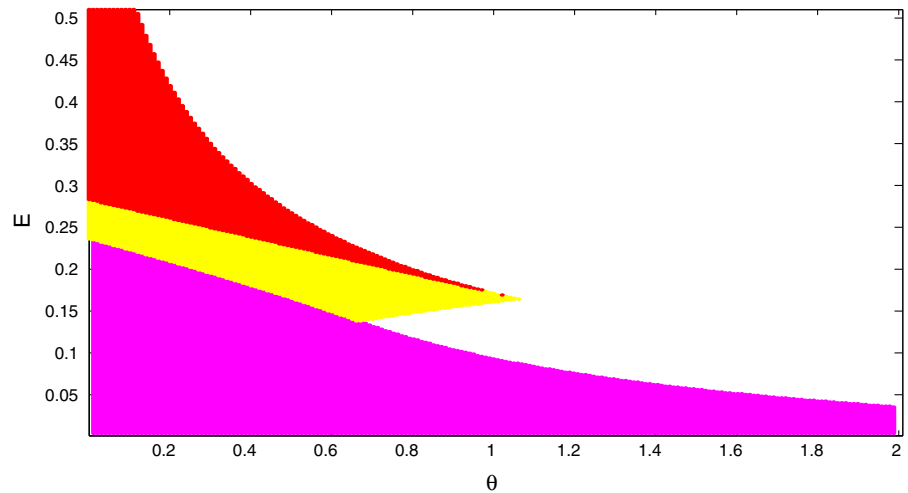


Table 3 Sufficient condition for bistability for system (5)

Attractor(s)	Sufficient condition	Biological implications
$E^0 \cup E_1^1$	E^0 is always stable; E_1^1 is stable for $1 > q_1 E$, $\beta S_1 < \mu + q_2 E$, $(1 - q_1 E)^2 > 4q_1 E\theta$ and $q_1 E + \frac{S_1^2}{S_1 + \theta} > (1 - S_1)(1 - \frac{\theta^2}{(S_1 + \theta)^2})$.	No interior equilibrium; here, we observe that this type of bistability occurs depending on the harvesting effort and Allee parameter (see Fig. 3a)
$E^0 \cup E^2$	E^0 is always stable; E^2 is stable for $\frac{\mu + q_2 E}{\beta} (1 - \frac{\mu + q_2 E}{\beta}) > q_1 E \frac{\mu + q_2 E}{\beta} + q_1 E\theta$, $-\frac{S_2^2}{S_2 + \theta} - \beta I_2 + \frac{(1 - S_2 - I_2)S_2(S_2 + 2\theta)}{(S_2 + \theta)^2} < q_1 E$ and $\alpha I_2 < d$.	No interior equilibrium; this type of bistability (see Fig. 3b) is very crucial as it is related to all species or predator extinction depending on the initial conditions
$E^0 \cup E_2^*$	E^0 is always stable; E_2^* exists if $S_2^* > \frac{\mu + q_2 E}{\beta}$, $B_{11}^2 > 4C_{11}$ and $(1 - (\beta + 1)\frac{d}{\alpha} - q_1 E) > 0$.	Different initial conditions lead to all species coexistence or extinction (see Fig. 3c)

ing on the parameter space), or converges to E_0 or E_2^* when interior equilibrium exists. We summarize the bistability criterion of the system (5) as follows (also see Table 3).

Note: Role of Allee effect on the existence of interior attractor of (5): Without Allee effect, the system (5) has one interior equilibria which is always stable (proof is not given), while in the presence of the Allee effect the system (5) can have either two interior equilibria or no equilibria, depending on the Allee parameter θ . So, from the above-described dynamics, we can conclude that Allee effect can generate or destroy interior attractors.

4 Mathematical analysis of the time delayed model (4)

In this section, we have analyzed the model (4). Here, we have performed permanence, local stability analysis of equilibria, the direction and stability of Hopf bifurcation of the delay differential Eq. (4).

4.1 Uniform persistence of the system

We first present the conditions for uniform persistence of the system (4). We denote by $\mathbb{R}_+^3 = \{(S, I, P) \in \mathbb{R}^3 : S \geq 0, I \geq 0, P \geq 0\}$ the non-negative quadrant

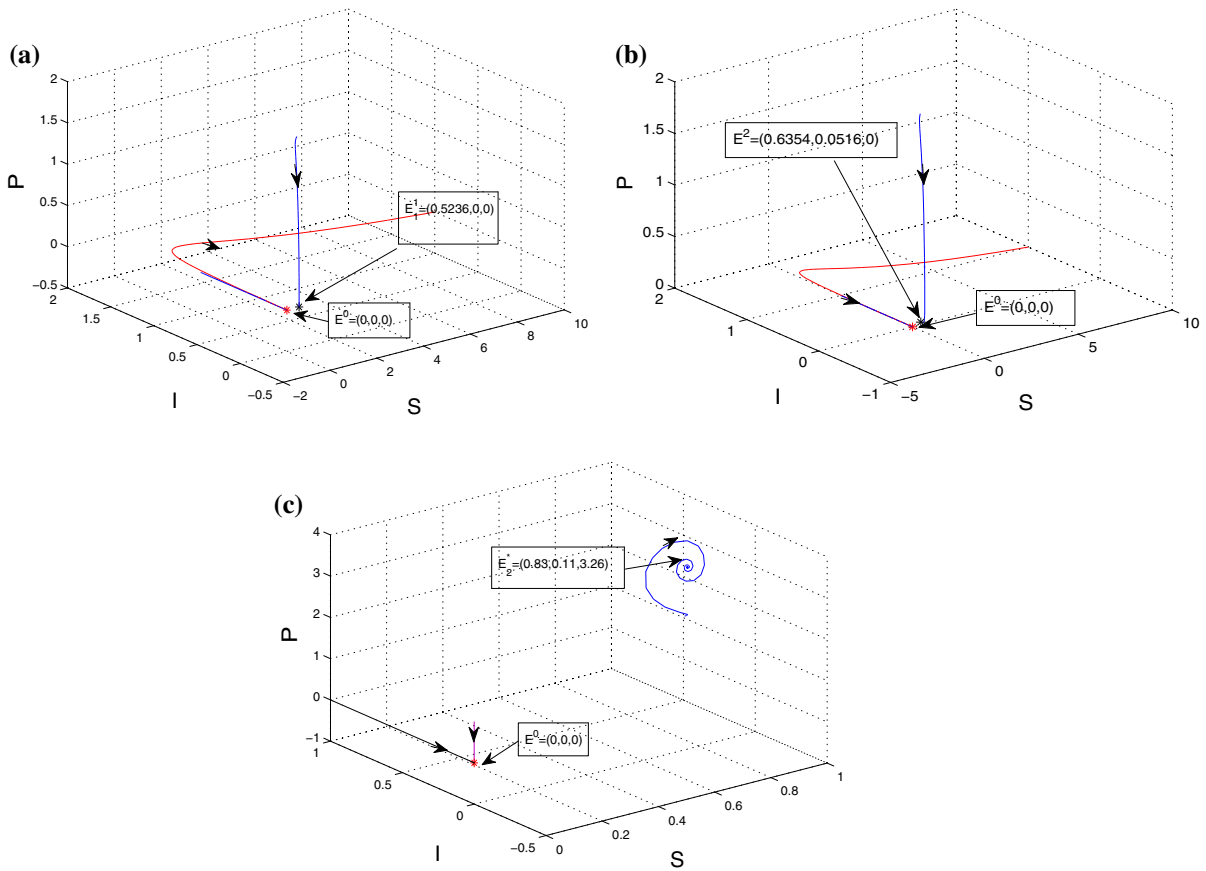


Fig. 3 **a** Bistability between E^0 and E^1 , **b** bistability between E^0 and E^2 and **c** bistability between E^0 and E_2^*

and by $\text{int}(\mathbb{R}_+^3) = \{(S, I, P) \in \mathbb{R}^3 : S > 0, I > 0, P > 0\}$.

Definition System (4) is said to be uniformly persistent if a compact region $D \subset \text{int}(\mathbb{R}_+^3)$ exists such that every solution $\mathcal{E}(t) = (S(t), I(t), P(t))$ of the system (4) with initial conditions eventually enters and remains in the region D .

4.2 Boundedness of the solution of the delayed system (4)

The first equation of the system (4) can be written as $\frac{dS}{dt} = \left[(1 - S - I) \frac{S}{S+\theta} - \beta I - q_1 E \right] dt$.

Integrating between the limits 0 and t , we have

$$S(t) = S(0) \exp \left\{ \int_0^t \left[(1 - S - I) \frac{S}{S+\theta} - \beta I - q_1 E \right] ds \right\}.$$

Similarly from the second and the third equation of the system, we have

$$I(t) = I(0) \exp \left\{ \int_0^t [\beta S - aP - \mu - q_2 E] ds \right\}$$

and

$$P(t) = P(0) \exp \left\{ \int_0^t \left[\alpha I(s - \tau) P(s - \tau) \frac{1}{P(s)} - d \right] ds \right\}$$

where $S(0) = S_0 > 0, I(0) = I_0 > 0$ and $P(0) = P_0 > 0$. Therefore, $S(t) > 0, I(t) > 0$ and $P(t) > 0$.

Proposition 2 All the solutions of the system (4) starting in $\text{int}(\mathbb{R}_+^3)$ are uniformly bounded with an ultimate bound.

For detailed proof see ‘‘Appendix.’’

4.3 Permanence

We use the uniform persistence theory for infinite dimensional systems [26], to prove permanence of the

system (4). Let X be a complete metric space. Suppose that X^0 is open and dense in X and $X^0 \cap X_0 = \Phi$. Assume that $T(t)$ is a C^0 semigroup on X satisfying

$$T(t) : X^0 \rightarrow X^0, T(t) : X_0 \rightarrow X_0. \tag{7}$$

Let $T_b(t) = T(t)|_{X_0}$ and let A_b be the global attractor for $T_b(t)$. To investigate the permanence of the system (4), the following lemmas are useful.

Lemma 1 [26] *If $T(t)$ satisfies (7) and we have the following:*

- (i) *there is a $t_0 \geq 0$ such that $T(t)$ is compact for $t \geq t_0$;*
- (ii) *$T(t)$ is a point dissipative in X ;*
- (iii) *$\widehat{A}_b = \cup_{x \in A_b} \omega(x)$ is isolated and thus has an acyclic covering \widehat{M} , where $\widehat{M} = \{M_1, M_2, \dots, M_n\}$;*
- (iv) *$W^s(M_i) \cap X^0 = \Phi$ for $i = 1, 2, \dots, n$.*

Then X_0 is a uniform repeller with respect to X^0 , i.e., there is an $\epsilon > 0$ such that for any $x \in X^0$, $\liminf_{t \rightarrow \infty} d(T(t)x, X_0) \geq \epsilon$, where d is the distance of $T(t)x$ from X_0 .

Lemma 2 [62] *Consider the following differential equation:*

$$\dot{x}(t) = Ax(t - \tau) - Bx(t)$$

where $A, B, \tau > 0$; $x(t) > 0$, for $-\tau \leq t \leq 0$. Then we have

- (i) *if $A < B$, then $\lim_{t \rightarrow \infty} x(t) = 0$;*
- (ii) *if $A > B$, then $\lim_{t \rightarrow \infty} x(t) = +\infty$.*

Theorem 1 (Permanence of the model (4)) *System (4) is permanent provided*

- (i) $\frac{\mu+q_2E+a\epsilon_1}{\beta} (1 - \frac{\mu+q_2E+a\epsilon_1}{\beta}) > q_1E \frac{\mu+q_2E+a\epsilon_1}{\beta} + q_1E\theta$, *where ϵ_1 is sufficiently small and*
- (ii) $\alpha(I_2 - \epsilon_2) > d$ *where $I_2 = \frac{(\frac{\mu+q_2E}{\beta})(1 - \frac{\mu+q_2E}{\beta}) - q_1E \frac{\mu+q_2E}{\beta} - q_1E\theta}{\frac{\mu+q_2E}{\beta} + \beta\theta + \mu + q_2E}$.*

Proof We have not given the detailed proof in this manuscript (our analysis is similar to the analysis given in [10]). □

4.4 Local stability analysis

Let $\tilde{E} = (\tilde{S}, \tilde{I}, \tilde{P})$ be any equilibrium point of the system (4). The linearized system of the system (4) at

$\tilde{E} = (\tilde{S}, \tilde{I}, \tilde{P})$ is

$$\begin{aligned} \dot{x}(t) &= \frac{(\beta\theta\tilde{I}-\tilde{S}^2)}{\tilde{S}+\theta}x(t) - \frac{\tilde{S}}{\tilde{S}+\theta}(\beta\theta + \tilde{S}(1 + \beta))y(t), \\ \dot{y}(t) &= \beta\tilde{I}x(t) - a\tilde{I}z(t), \\ \dot{z}(t) &= y(t - \tau)\alpha\tilde{P} + z(t - \tau)\alpha\tilde{I} - dz(t). \end{aligned} \tag{8}$$

So, the characteristic equation of the delayed system (4) around any equilibrium point $\tilde{E} = (\tilde{S}, \tilde{I}, \tilde{P})$ is given by

$$\det \begin{bmatrix} \frac{(\beta\theta\tilde{I}-\tilde{S}^2)}{\tilde{S}+\theta} - \lambda - \frac{\tilde{S}}{\tilde{S}+\theta}(\beta\theta + \tilde{S}(1 + \beta)) & 0 & 0 \\ \beta\tilde{I} & -\lambda & -a\tilde{I} \\ 0 & e^{-\lambda\tau}\alpha\tilde{P} & e^{-\lambda\tau}\alpha\tilde{I} - d - \lambda \end{bmatrix} = 0. \tag{9}$$

In previous section, we observe that in the absence of the delay, the interior equilibrium $E_1^* = (S_1^*, I_1^*, P_1^*)$ is unstable, while the other interior equilibria $E_2^* = (S_2^*, I_2^*, P_2^*)$ is locally stable. Hence, in the present section, we study the stability analysis of the delayed system around the interior equilibria E_2^* .

The following transcendental equation represents the characteristic equation at the interior equilibrium $E_2^* = (S_2^*, I_2^*, P_2^*)$ of the dynamical system (4).

$$\lambda^3 + B_1\lambda^2 + B_2\lambda + B_3 = [B_4\lambda^2 + B_5\lambda + B_6]e^{-\lambda\tau}. \tag{10}$$

where

$$\begin{aligned} B_1 &= -\frac{(\beta\theta I_2^* - S_2^{*2})}{S_2^* + \theta} + d, \\ B_2 &= -\frac{(\beta\theta I_2^* - S_2^{*2})}{S_2^* + \theta}d \\ &\quad + \beta I_2^* \frac{S_2^*}{S_2^* + \theta}(\beta\theta + S_2^*(1 + \beta)), \\ B_3 &= \beta I_2^* \frac{S_2^*}{S_2^* + \theta}(\beta\theta + S_2^*(1 + \beta))d, \\ B_4 &= \alpha I_2^*, \\ B_5 &= -\alpha I_2^* \frac{(\beta\theta I_2^* - S_2^{*2})}{S_2^* + \theta} - \alpha\alpha I_2^* P_2^*, \\ B_6 &= \beta\alpha I_2^* I_2^* \frac{S_2^*}{S_2^* + \theta}(\beta\theta + S_2^*(1 + \beta)) \\ &\quad + \alpha\alpha I_2^* P_2^* \frac{(\beta\theta I_2^* - S_2^{*2})}{S_2^* + \theta}. \end{aligned} \tag{11}$$

For the delay induced system (4), it is known that if all the roots of the corresponding characteristic equation (10) have negative real part, then the equilibrium point E_2^* will be asymptotically stable. The classical

Routh–Hurwitz criterion cannot be used to determine the stability of the dynamical system as the characteristic equation (10) is a transcendental equation and has infinitely many roots. We need the sign of the real parts of the roots of the characteristic equation (10), to investigate the nature of the stability.

Let $\lambda(\tau) = \zeta(\tau) + i\rho(\tau)$ be the eigenvalue of the characteristic equation (10); substituting this value in Eq. (10), we obtain real and imaginary parts, respectively, as

$$\begin{aligned} &\zeta^3 - 3\zeta\rho^2 + B_1(\zeta^2 - \rho^2) + B_2\zeta + B_3 \\ &= \left[\left\{ B_4(\zeta^2 - \rho^2) + B_5\zeta + B_6 \right\} \right. \\ &\quad \left. \cos \rho\tau (2B_4\zeta\rho + \rho B_5) \sin \rho\tau \right] e^{-\zeta\tau}, \end{aligned} \tag{12}$$

and

$$\begin{aligned} &3\zeta^2\rho - \rho^3 + 2B_1\zeta\rho + B_2\rho \\ &= [(2B_4\zeta\rho + B_5\rho) \cos \rho\tau \\ &\quad - \{(\zeta^2 - \rho^2) B_4\zeta B_5 + B_6\} \sin \rho\tau] e^{-\zeta\tau}. \end{aligned} \tag{13}$$

A necessary condition to change the stability of E_2^* is that the characteristic equation (10) should have purely imaginary solutions. We set $\zeta = 0$ in (12) and (13). Then we get,

$$B_3 - B_1\rho^2 = (-B_4\rho^2 + B_6) \cos \rho\tau + \rho B_5 \sin \rho\tau, \tag{14}$$

$$B_2\rho - \rho^3 = B_5\rho \cos \rho\tau - (-B_4\rho^2 + B_6) \sin \rho\tau. \tag{15}$$

Eliminating τ by squaring and adding the equations (14) and (15), we get the algebraic equation for determining ρ as

$$\begin{aligned} &\rho^6 + (B_1^2 - 2B_2 - B_4^2) \rho^4 \\ &+ (B_2^2 - 2B_1B_3 - B_5^2 + 2B_4B_6) \rho^2 \\ &+ (B_3^2 - B_6^2) = 0. \end{aligned} \tag{16}$$

Substituting $\rho^2 = \theta$ in Eq. (16), we obtain a cubic equation given by

$$k(\theta) = \theta^3 + \sigma_1\theta^2 + \sigma_2\theta + \sigma_3 = 0, \tag{17}$$

where

$$\begin{aligned} \sigma_1 &= (B_1^2 - 2B_2 - B_4^2), \quad \sigma_2 \\ &= (B_2^2 - 2B_1B_3 - B_5^2 + 2B_4B_6), \quad \sigma_3 \\ &= (B_3^2 - B_6^2). \end{aligned}$$

Now $\sigma_3 < 0$ implies that (17) has at least one positive root. The following theorem gives a criterion for the switching in the stability behavior of E_2^* .

Theorem 2 *Suppose that E_2^* exists and is locally asymptotically stable for (4) with $\tau = 0$. Also let $\theta_0 = \rho_0^2$ be a positive root of (17).*

1. *Then there exists $\tau = \tau^*$ such that the interior equilibrium point E_2^* of the delay system (4) is asymptotically stable when $0 \leq \tau < \tau^*$ and unstable for $\tau > \tau^*$.*
2. *Furthermore, the system will undergo a Hopf bifurcation at E_2^* when $\tau = \tau^*$, provided $Z(\rho)X(\rho) - Y(\rho)W(\rho) > 0$.*

Proof The proof is similar to the analysis given in [10]. □

4.5 The direction and stability of Hopf bifurcating periodic solutions

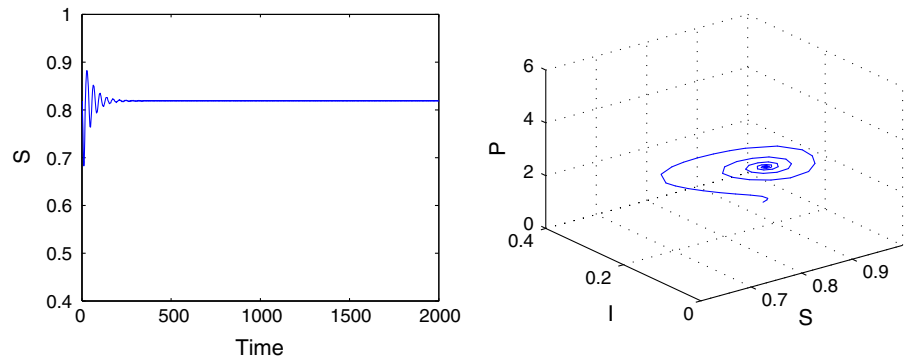
We already know that the system (4) will undergo Hopf bifurcation at endemic equilibrium $E_* = (S_*, I_*, P_*)$ when τ passes through τ^* (for our convenience we assume that $E_* = E_2^*$). In this section, we investigate the direction, stability and period of Hopf bifurcating solutions at $\tau = \tau^*$ for system (4) by using the techniques of normal form theory and center manifold theorem introduced by [27].

We have not given the detailed analysis for the direction and stability of the Hopf bifurcation in this manuscript (our analysis is similar to the analysis given in [10]). From the detailed analysis, we can compute the following quantities, which determine the direction, stability and the periods of the bifurcating periodic solutions of Hopf bifurcation.

$$\begin{aligned} C_1(0) &= \frac{i}{2\rho_0\tau^*} \left(g_{20}g_{11} - 2|g_{11}|^2 - \frac{1}{3}|g_{02}|^2 \right) + \frac{1}{2}g_{21}, \\ \mu_2 &= -\frac{Re\{C_1(0)\}}{Re\{\hat{\lambda}(\tau^*)\}}, \\ \beta_2 &= 2Re\{C_1(0)\}, \\ \tau_2 &= -\frac{Im\{C_1(0)\} + \mu_2 Im\{\hat{\lambda}(\tau^*)\}}{\rho_0\tau^*}. \end{aligned}$$

It is well known that μ_2 and β_2 determine the direction of Hopf bifurcation and stability of bifurcating periodic solutions. If $\mu_2 > 0$ (< 0), and $\beta_2 < 0$ (> 0), then the Hopf bifurcation is supercritical (subcritical),

Fig. 4 Waveform plot and phase plane for the delayed system (4), with the time delay $\tau = 1 (< \tau_* = 3.2)$ and the other parameter values are fixed as in Table 1. The first row left figure is the time series for the susceptible prey; the first row right figure is the 3D phase portrait of the stable interior of (4)



bifurcating periodic solutions exist for $\tau > \tau^*$ ($\tau < \tau^*$) and are orbitally stable (unstable). τ_2 determines the periods of the bifurcating periodic solutions and the period increases (decreases) if $\tau_2 > 0 (< 0)$.

From our analytical findings, it is observed that E_2^* is locally asymptotically stable for $\tau < \tau^* = 3.20$. Figure 4 shows that the system (4) is stable focus for $\tau = 1 < \tau^*$. Interior equilibrium point E_2^* loses its stability as τ passes through its critical value τ^* and the system (4) experiences Hopf bifurcation. From 4.5, the nature of the stability and direction of the periodic solution bifurcating from the interior equilibrium E_2^* at the critical point τ^* can be computed. Through simulations, we compute that

$$C_1(0) = -3.4661 - 0.9500i, \mu_2 = 588.89, \\ \beta_2 = -6.9323, \tau_2 = 11.972.$$

It shows the existence of bifurcating periodic solution, and it is supercritical and stable as evident from Fig. 5. Figure 5 shows that the limit cycle is stable around the coexisting equilibrium point E_2^* . The solutions starting from two different initial values converge to the limit cycle oscillation for $\tau = 3.28$.

5 Chaotic behavior in our model dynamics (4)

In this section, the time series diagram, phase plane diagram and bifurcation diagram of the system (4) are drawn to describe the feasibility of different complex dynamical behaviors such as one periodic and two periodic limit cycles and chaos.

We fix the parameter values as in Table 1 and vary the time delay parameter to investigate the different complex dynamics of our model (4). For our model (4), the equilibrium E_2^* is locally asymptotically stable for the delay parameter $\tau < 3.20 (= \tau^*)$. If we increase

the parameter beyond τ^* , then at $\tau = 4 > \tau_*$, the system (4) shows the limit cycle oscillation of period one (see Fig. 6). If we further increase the time delay parameter τ , then the system (4) will show the limit cycle oscillation of period two for $\tau = 11.2$ (see Fig. 7).

We observe that system (4) shows the chaotic behavior for $\tau = 18$ (see Fig. 8). To establish the chaotic dynamics, we have plotted the maximum Lyapunov exponent with time in Fig. 9a, corresponding to Fig. 8. We use Wolf algorithm [61] to calculate maximum Lyapunov exponents. A Poincare map of a typical chaotic regime is shown in Fig. 9b. The scattered distribution of the sampling points implies the chaotic behavior of the system.

6 Effects of the time delay (τ), inverse of individual searching efficiency (θ) and harvesting effort (E)

In this section, we will discuss the effects of the three important model parameters: (a) effects of time lag τ , (b) effects of the inverse of individual searching efficiency θ and (c) the effects of the harvesting effort. We produce three bifurcation diagrams with respect to τ , θ and E for our model (4) to clearly depict our results, by fixing the other parameter values as in Table 1.

6.1 Effect of time lag

First we draw the bifurcation diagram with respect to time delay τ for $0 < \tau \leq 18.5$, with the parameter values $\theta = 0.1, E = 0.01$ and the remaining parameters are fixed as in Table 1. The bifurcation diagram with respect to time delay τ drawn in Fig. 10 reports the complex dynamical behavior of the model (4) with period doubling bifurcation. The system (4)

Fig. 5 The system (4) shows Hopf bifurcation behavior and existence of stable supercritical bifurcating periodic solution around the interior equilibrium E_2^* at $\tau = 3.28$. The other parameter values are kept same as in Table 1

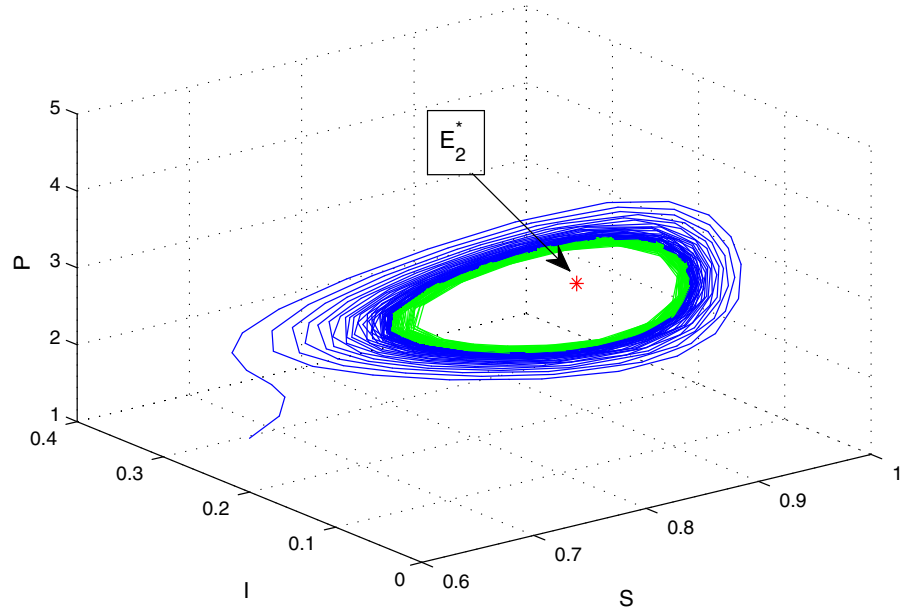


Fig. 6 Waveform plot and phase plane for the delayed system (4), with the time delay $\tau = 4$ and the other parameter values are fixed as in Table 1. Figure indicates the existence of limit cycle

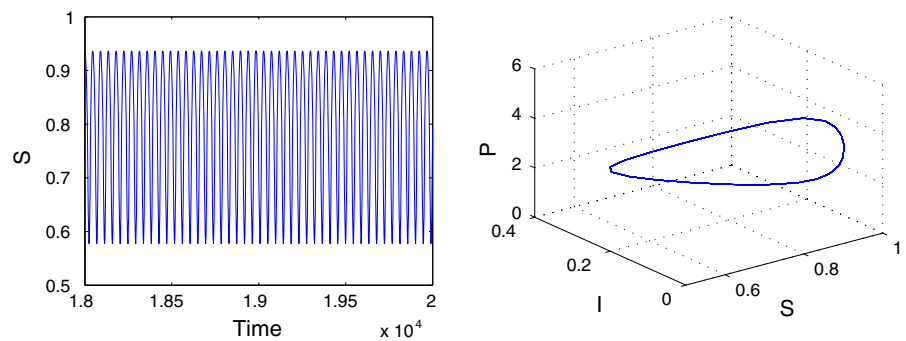
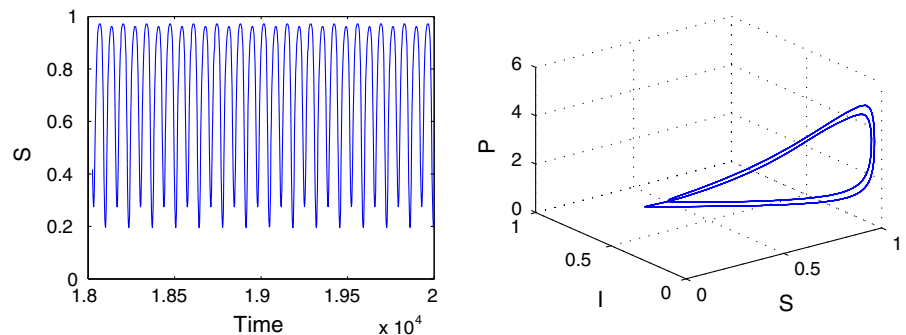


Fig. 7 Existence of two periodic solutions around the interior equilibrium E_2^* for the system (4), with the time delay $\tau = 11.4 (> \tau^* = 3.2)$, where the other parameter values are same as in Table 1



undergoes from stable focus to limit cycle oscillation, limit cycle oscillation to chaotic oscillation for further increase the delay parameter. Figure 10 shows that for $\tau \in [0, 3.2)$ the interior equilibrium E_2^* is stable, for $\tau \in [3.2, 11.2)$ it shows limit cycle oscillations, and for $\tau \in [11.2, 18.5)$ it exhibits higher periodicity and chaotic oscillations.

6.2 Effect of Allee parameter

Next, we draw the bifurcation diagram with respect to the parameter θ for $\theta \in (0, 1.28]$ where τ is fixed at 18, $E = 0.01$ and the remaining parameters are fixed as above. The complex dynamic behavior including chaos of the delayed system with respect to θ is evi-

Fig. 8 Solution curves and the phase plane showing chaotic attractor at $\tau = 18$ for the model (4) and the other parameter values are fixed as in Table 1

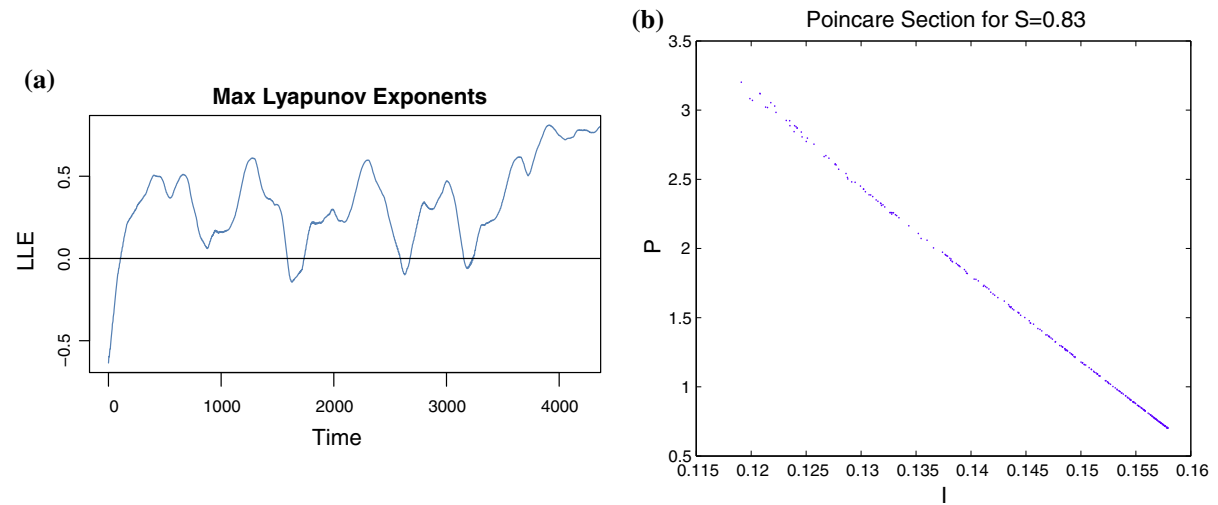
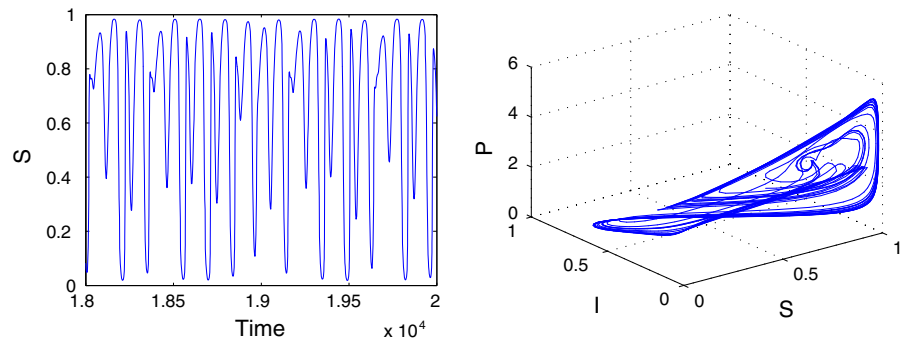


Fig. 9 Maximum Lyapunov exponents and Poincare section to show the chaotic behavior of the system (4). **a** Chaotic behavior of the system (4). **b** Poincare plot $\{S=0.83\}$ in the I–P plane for the system (4)

dent from Fig. 11. We observe that for $\theta \in (0, 0.05)$, system exhibits limit cycle and for $\theta \in [0.05, 0.44)$ the system (4) shows higher periodicity and chaotic oscillations through quasi-periodicity route. For further increasing the strength of Allee parameter invokes a period-halving bifurcation and controls the chaotic oscillations. The system (4) shows two-period oscillation and limit cycle behavior for $\theta \in (0.44, 0.78)$, and $\theta \in (0.78, 1.28]$, respectively. Further increment of θ results extinction of all the species.

6.3 Effect of harvesting effort

We fix the parameter values $\tau = 18, \theta = 0.1$ and the other parameters are fixed as above and vary the parameter E. For the gradual increase of the parameter E,

the system (4) switches its stability from chaotic oscillation to limit cycle oscillation, limit cycle oscillation to stable focus through the period-halving bifurcation. When $E \in [0, 0.04)$, we observe higher periodicity and chaotic oscillations. For $E \in [0.04, 0.1)$, we notice limit cycle behavior. Figure 12 shows that the system is stable for $E \in [0.10, 0.15]$.

For clear visualization, we draw the stability region for the model (4), with respect to θ and E when $\tau = 18$. In Fig. 13, the whole region is divided into several distinct parts where we observe that the system (4) is stable in the green region; black region shows limit cycle oscillation, period doubling in the yellow region, chaotic oscillation in the blue region; predator extinction in the red region, infected prey and predator extinction in the cyan region and white region shows the extinction of all species.

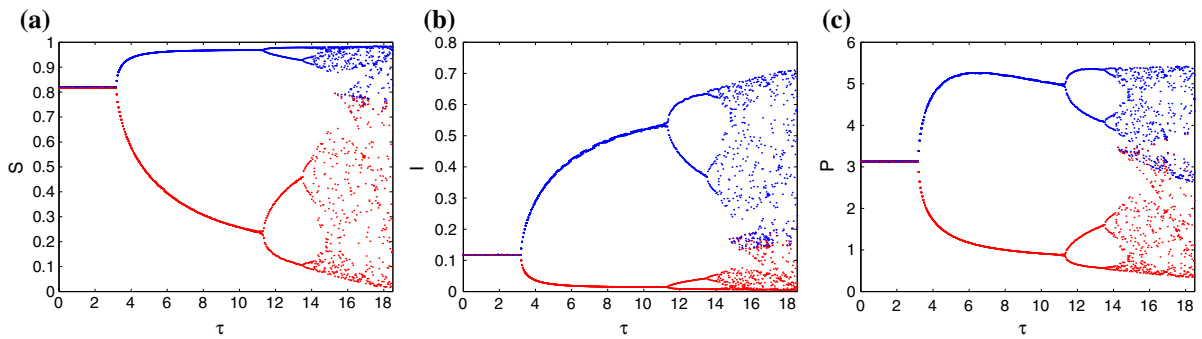


Fig. 10 Bifurcation diagrams with respect to τ for the system (4), when the other parameters are fixed as in Table 1. **a** Bifurcation diagram for the susceptible prey; **b** bifurcation diagram for the infected prey; and **c** bifurcation diagram for the predator

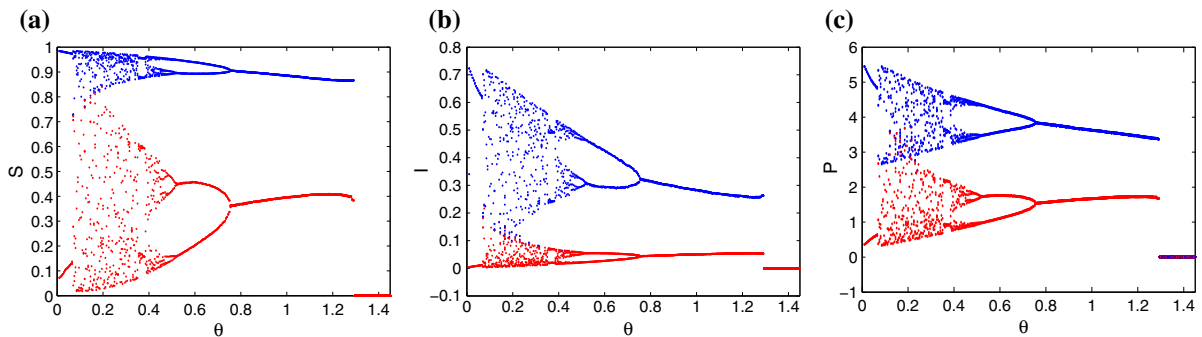


Fig. 11 Bifurcation diagrams with respect to θ for the system (4). When the other parameters are fixed as in Table 1 and $\tau = 18$. **a** Bifurcation diagram for the susceptible prey; **b** bifurcation diagram for the infected prey; and **c** bifurcation diagram for the predator

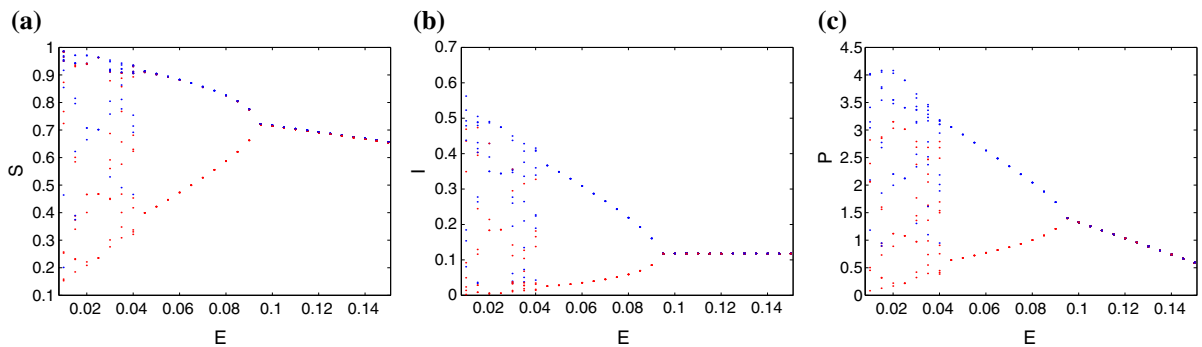


Fig. 12 Bifurcation diagrams with respect to E for the system (4). When the other parameters are fixed as in Table 1 and $\tau = 18$. **a** Bifurcation diagram for the susceptible prey; **b** bifurcation diagram for the infected prey; and **c** bifurcation diagram for the predator

7 Optimal harvesting policy

In this section, we study the optimal harvesting policy for both the non-delayed and delayed model. Exploitation can change the behavior of the system in several ways. It can reduce population size or density to a level close to or below an Allee threshold or

increases the Allee effect strength. For example, in an Irish sea, at least four species of skate and shark have been exploited to extinction [6]. Naturally optimal harvesting policy is very much needed for such system. So, we formulate an optimal harvesting policy which ensures species conservation and maximizes the profit [23,33,36].

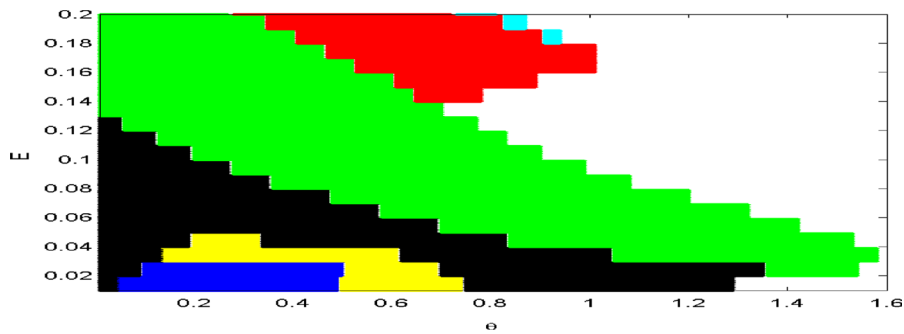


Fig. 13 Stability region of the system (4) when $\tau = 18$. The system is stable in the *green region*, *black region* shows limit cycle oscillation, period doubling in the *yellow region*, chaotic oscillation in the *blue region*, predator extinction in the *red region*, infected prey and predator extinction in the *cyan region* and *white region* shows the extinction of all species

lation in the blue region, predator extinction in the *red region*, infected prey and predator extinction in the *cyan region* and *white region* shows the extinction of all species

Here, we study the optimal harvesting policy by considering the profit earned by harvesting with conservation of prey population. We assume that price function is inversely proportional to the available prey population. Let c be the constant harvesting cost per unit effort, p_1 and p_2 are constant price per unit biomass of the S and I species, v_1 and v_2 are economic constraints and δ denotes the continuously compounded annual rate of discount. Infected prey (I) has less demand, so we assume that $p_2 < p_1$.

We now formulate the problem of optimal harvesting policy for

$$J(E) = \int_0^T [(p_1 - v_1 q_1 E S) q_1 E S + (p_2 - v_2 q_2 E I) q_2 E I - c E] e^{-\delta t} dt,$$

subject to the system (4) and the effort constraint $0 \leq E \leq E_{\max}$. Here, E_{\max} is the maximum effort capacity of the harvesting industry. The objective of the problem is to find the optimal harvesting effort E^* such that

$$J(E^*) = \max_{E \in U} J(E)$$

where U is the control set defined by

$$U = \{E : E \text{ is measurable and } 0 \leq E \leq E_{\max}\}.$$

To find the maximum value of $J(E)$, we set $x(t) = (S(t), I(t), P(t))$ and $x_\tau(t) = (S_\tau(t), I_\tau(t), P_\tau(t))$, where $S_\tau(t) = S(t - \tau)$, $I_\tau(t) := I(t - \tau)$, $P_\tau(t) := P(t - \tau)$, and define the Hamiltonian $H(t) = H(x, x_\tau, E, \lambda)(t)$ for the control problem as follows:

$$H = [(p_1 - v_1 q_1 E S) q_1 E S + (p_2 - v_2 q_2 E I) q_2 E I - c E] + \lambda_S \left[S \left[(1 - S - I) \frac{S}{(S + \theta)} - \beta I - q_1 E \right] \right] + \lambda_I [I [\beta S - a P - \mu - q_2 E]] + \lambda_P [\alpha P(t - \tau) I(t - \tau) - d P].$$

The variables $\lambda_S, \lambda_I, \lambda_P$ are adjoint variables and the transversality conditions are $\lambda_S(T) = 0, \lambda_I(T) = 0$ and $\lambda_P(T) = 0$.

Theorem 3 *There exists an optimal control E^* for $t \in [0, T]$ such that*

$$J(S(t), I(t), P(t), E^*) = \max_{E \in U} J(S(t), I(t), P(t), E)$$

subject to the differential equation (4) and there exists adjoint variables $\lambda_S, \lambda_I, \lambda_P$ with the transversality conditions as $\lambda_S(T) = 0, \lambda_I(T) = 0, \lambda_P(T) = 0$.

Proof For details, see [23,32,33,36]. □

7.1 Characterization of the optimal control

In order to derive the necessary condition for the optimal control, Pontryagin's maximum principal with delay given in [68] was used. The state equations are given by:

$$x(t) = H(x, x_\tau, E, \lambda)(t),$$

the optimality condition is

$$0 = H_E(x, x_\tau, E, \lambda)(t),$$

and the adjoint equation is

$$-\frac{d\lambda}{dt}(t) = H_x(x, x_\tau, E, \lambda)(t) + \chi_{[0, T-\tau]} \lambda(t + \tau) H_{x_\tau}(x, x_\tau, E, \lambda)(t),$$

where H_E, H_x and H_{x_τ} denote the derivative with respect to E, x and x_τ , respectively. Now we apply the necessary conditions to the Hamiltonian H .

The condition for the optimal control can be obtained from the relation $E_\delta = \frac{p_1 q_1 S + p_2 q_2 I - c - \lambda_S q_1 S - \lambda_I q_2 I}{2(v_1 q_1^2 S^2 + v_2 q_2^2 I^2)}$. The adjoint equations are

$$\begin{aligned} \frac{d\lambda_S}{dt} &= \lambda_S(t)\delta - [p_1 q_1 E - 2v_1 q_1^2 E^2 S] \\ &\quad - \lambda_S(t) \left[S(1 - S - I) \frac{(S + 2\theta)}{(S + \theta)^2} - \frac{S^2}{S + \theta} - \beta I - q_1 E \right] \\ &\quad - \lambda_I(t)\beta I \\ \frac{d\lambda_I}{dt} &= \lambda_I(t)\delta - [p_2 q_2 E - 2v_2 q_2^2 E^2 I] \\ &\quad + \lambda_S(t)\beta S - \lambda_I(t) [\beta S - aP - \mu - q_2 E] \\ &\quad - \chi_{[0, T-\tau]} \lambda_P(t + \tau) \alpha P(t - \tau) \\ \frac{d\lambda_P}{dt} &= \lambda_P(t)\delta - \lambda_P(t)d \\ &\quad + \lambda_I(t)aI - \chi_{[0, T-\tau]} \lambda_P(t + \tau) \alpha I(t - \tau) \end{aligned} \tag{18}$$

The optimal harvesting effort at any time t is given by

$$E^* = \begin{cases} E_{\min}, & \frac{dH}{dE} < 0 \\ E_\delta, & \frac{dH}{dE} = 0 \\ E_{\max}, & \frac{dH}{dE} > 0. \end{cases} \tag{19}$$

The numerical solutions of the considered optimal problem completely determined using Runge–Kutta fourth-order forward–backward procedure. The successive steps are displayed as follows:

Let there exists a step size $h > 0$ and $\tau = mh, T = nh$. We obtain the following partition: $t_{-m} < -\tau < \dots < t_0 < \dots < T < \dots < t_{n+m}$. Then we have $t_i = t_0 + ih$.

1. For $i = -m, \dots, 0$ do $S_i = S_0; I_i = I_0; P_i = P_0; E^*_i = 0$ End for
For $i = n, \dots, n + m$ do $\lambda_S = 0; \lambda_I = 0; \lambda_P = 0$ End for
2. For $i = 0, \dots, n - 1$ using the initial condition S_0, I_0, P_0 solve the state equation according to the

DDE with the values for E^* forwardly.

Using the transversality condition $\lambda_S(T) = 0, \lambda_I(T) = 0, \lambda_P(T) = 0$, with the computed values of state variables and E^* evaluate the values of adjoint variables $\lambda_S, \lambda_I, \lambda_P$.

3. Update E^* using the rule $E^* = \min\{E_{\min}, \max\{E_\delta, E_{\max}\}\}$.
4. If the solutions of the variables (excluding the control variable) are convergent then the last iteration is the complete solution. Otherwise, return to step 2.

We illustrate this with a numerical example. For this purpose, we choose the parameter values to be $\beta = 0.75; \mu = 0.001; d = 0.1; a = 0.4; \theta = 0.1; \alpha = 0.2; T = 10; \epsilon = 0.05; p_1 = 1.2; p_2 = 0.1; q_1 = 1; q_2 = 1; v_1 = 2; v_2 = 2; c = 0.1; S(0) = 1; I(0) = 0.05; P(0) = 1$. We assume that $0 \leq E \leq 1$. Now we solve the optimal control problem numerically using Runge–Kutta fourth-order iterative method. For the state variables, first we solve the system (5) by forward Runge–Kutta fourth-order procedure and then using that state values we solve the system (18) by using the backward fourth-order Runge–Kutta procedure (when $\tau = 0$).

In Fig. 14, we represent the solution curves of the three state variables in the presence of the harvesting. Figure 15 represents the variation of adjoint variables. Final values of the adjoint variables are 0. As harvesting effort increases, the biomass of prey and predator population decreases. From Fig. 16, we observe that the optimal harvesting effort is maximum when $\theta = 0.5$. The optimal effort E_δ varies with θ . Biologically, we can say that if θ increases, then numerically $\frac{S}{S+\theta}$ decreases and as a result maximum optimal harvesting effort increases.

Next, we assume the same parameter values as Fig. 14 and $0 \leq E \leq 1$. Using the above-described method in subsection 7.1, we investigate optimal harvesting policy for the model (4). For $\tau = 1$, the optimal trajectories for the system (4) with initial population densities $(S(0), I(0), P(0))$ are shown in Fig. 17. The variations of adjoint variables are also drawn in Fig. 18. Optimal harvesting effort is hugely dependent on gestation delay τ which is evident from Fig. 19. Maximum value of optimal harvesting increases as gestation delay τ increases. The optimal harvesting effort increases monotonically and assumes its maximum value in each case.

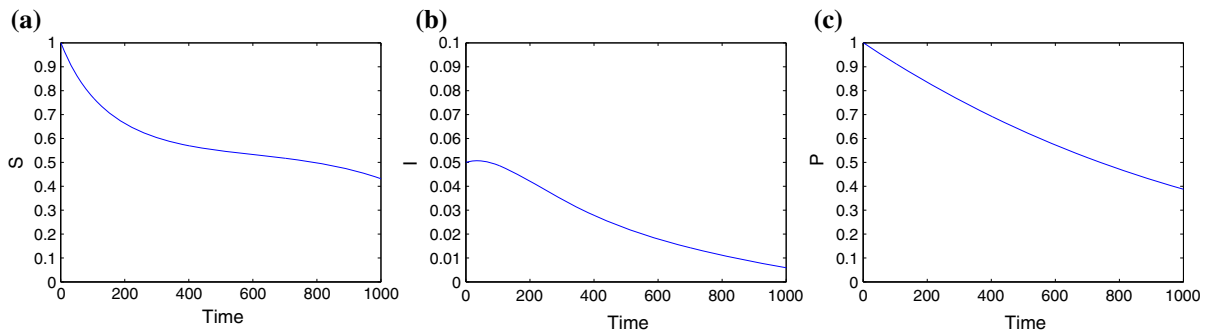


Fig. 14 Diagrams for the state variables with control for the system (5). **a** Diagram for the susceptible prey; **b** diagram for the infected prey; and **c** diagram for the predator

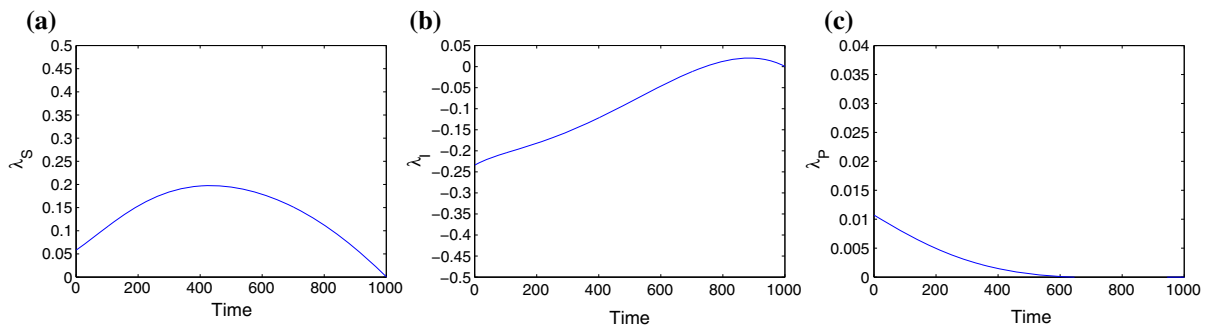


Fig. 15 Figures for the adjoint variables of the system (5)

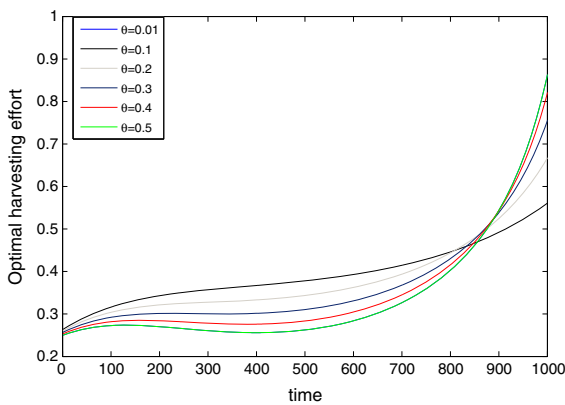


Fig. 16 Variation of the optimal effort E with respect to time with different θ for the system (5)

8 Discussion

The model (4) has two interior equilibria E_1^* and E_2^* , in which first one is always unstable and the another one is stable. We discuss the saddle node bifurcation and bistability between different equilibria for the model

(5). For our model (4), the delay parameter (τ) plays an important role. Time delay can switch the stability of the equilibrium point from stable to unstable; that is, for some critical value τ^* , the positive equilibrium E_2^* is stable when $\tau < \tau^*$, and it becomes unstable as τ crosses through its critical magnitude from lower to higher values. It is demonstrated that the model (4) encounters the Hopf bifurcation as the delay parameter τ crosses the critical value τ^* . Further increasing of the delay parameter beyond the bifurcation point leads to complex dynamic behavior, including chaos. The explicit formulae which determine the stability, direction and other properties of bifurcating periodic solution are investigated, by using normal form and center manifold theorem. Finally, by using numerical simulations, we illustrate our analytical results. We also draw the various stability regions for the model (4), with respect to θ and E when $\tau = 18$.

From environmental perspective, chaos has the most extreme natural significance. Numerous hypothetical studies uncover essential biological community’s highlight, for example, consistency, species constancy [2]

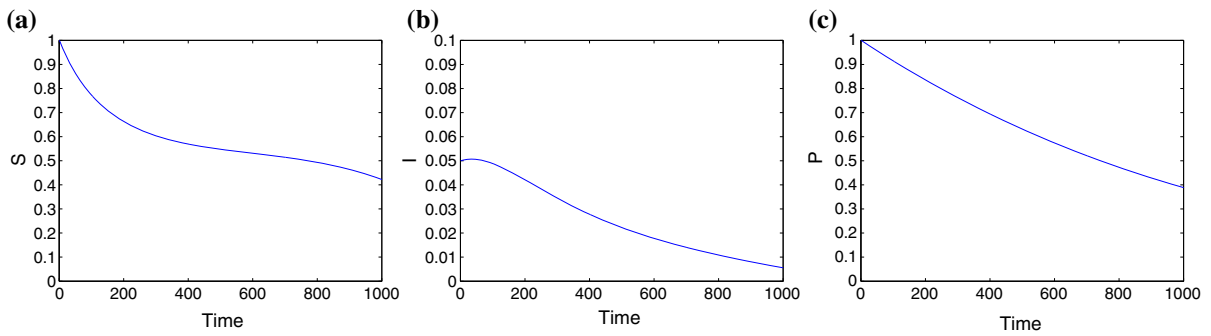


Fig. 17 Diagrams for the state variables with control for the system (4). **a** Diagram for the susceptible prey; **b** diagram for the infected prey; and **c** diagram for the predator

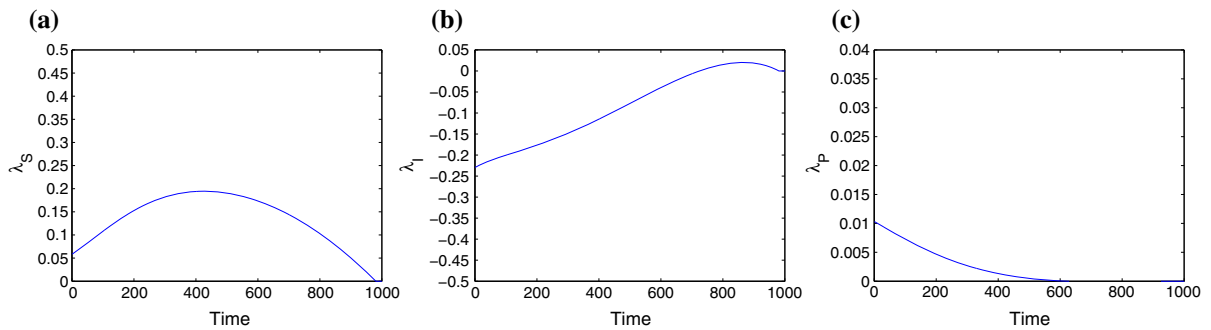


Fig. 18 Figures for the adjoint variables of the system (4) when $\tau = 1$

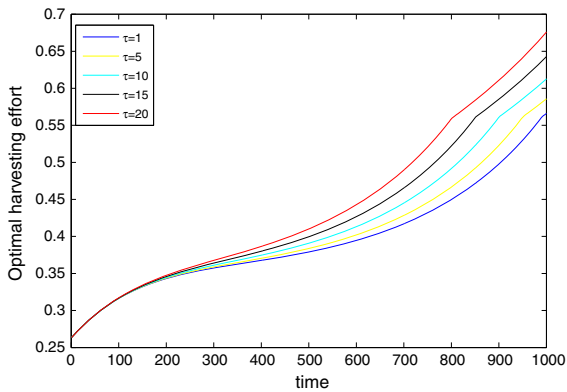


Fig. 19 Variation of the optimal effort E with respect to time with different τ for the system (4)

and bio-differences [31] can be influenced by chaos. Different chaos control plans have been investigated, till now. In [34, 53, 69], the authors concluded that Allee effect may be a destabilizing force in prey–predator systems. We have shown that higher values of time delay make the system chaotic, and chaos can be con-

trolled by the harvesting effort E . In our model (4), the non-linearity induced by Allee effect can produce chaotic oscillations but the changes in the strength of θ may reduce/remove the chaotic behavior of the system. The dynamical behavior of θ is not same as in [10]. Clearly, if the Allee parameter increases, the system loses stability and becomes chaotic. It is worth noting that we draw the bifurcation diagram by plotting the maximum and minimum values of the time series solutions of the system (4). We observe that the system (4) enters into the chaotic regime through quasi-periodicity route [50]. The impact of the Allee effect on the stability of population models show a diverse effect which entirely relies on the assumption of the relating model. Harvesting makes the coexistence equilibria stable for the system (4) and can control chaotic dynamics of the system. Continuous harvesting will make the system disease-free (also predator-free). The system has the ability to recover if P -class are not made extinct by excessive exploitation of their food supply.

We assume that the selling price of the infected prey (I) is less than the price of susceptible fish (S). Large

amount of infected prey is harmful for the economic condition of harvesters. Also if q_1 and q_2 increase with the advancement of technology, while the remaining parameters are fixed, then the density of prey population shifts to a lower level. Further increment of q_1 and q_2 makes the prey population extinct. In this article, we consider the economic loss of harvesters due to the unwilling harvesting of infected prey species. Using the *Pontryagin's maximum principle*, the optimal harvesting policy has been discussed. We find that optimal harvesting policy is dependent on both gestation delay and Allee effect.

A large number of empirical evidences for drastic global reduction of valuable fish stocks are available. In fisheries, undisciplined harvesting diminish the population at the point where depensatory process dominates. Long ago fishery scientists are acquainted with the possibility of Allee effects (depensatory) in marine populations [45] and demanded enquiry of the ‘‘depensatory process.’’ In fisheries, strong and weak Allee effects are known as critical and pure depensation, respectively [16]. First time we develop a management problem considering an eco-epidemiological model with weak Allee effect and harvesting in prey population. One practical example for our model (4) is Antarctic krill-whale community. The Antarctic krill population is being increasingly harvested and the prime source of food of whales is krill. We use gestation delay to make our model (4) more realistic. Exploitation can affect system with Allee effects in several ways. It can reduce population density to a level close to or below an Allee threshold or increase the Allee effect strength [6]. We observe that, for our model (4), prey density should be greater than $\frac{\mu+q_2E}{\beta}$ for existence of all the species. Effective harvesting helps to protect biological balance within the ecosystem which is our prime goal. Optimal harvesting policy is an important tool to maximize the profit earned by exploitation while ensuring the existence of all the species. Figures 14 and 17 indicate the existence of all the species with optimal harvesting policy. Our findings indicate that over exploitation implies the extinction of the population, and a proper harvesting policy should ensure the feasibility of the biomass which is in line with reality.

Acknowledgements SB’s and MD’s research are supported by the senior research fellowship from the University Grants Commission, Government of India. SKS’s and SS’s research works are supported by NBHM postdoctoral fellowship. JC’s research

is partially supported by a DAE project (Ref Nos. 2/48(4)/2010-R and D II/8870).

Appendix

We can write the first equation of the system (4) as

$$\frac{dS}{dt} = S \left[(1 - S - I) \frac{S}{S + \theta} - \beta I - q_1 E \right].$$

So,

$$\begin{aligned} \frac{dS}{dt} &\leq S(1 - S), \\ \therefore \limsup_{t \rightarrow \infty} S(t) &\leq 1. \end{aligned}$$

Let $V_1 = S + I$, taking its time derivative along the solution of the system (4), we have

$$\begin{aligned} \dot{V}_1 &= S(1 - S - I) \frac{S}{S + \theta} - aPI - \mu I - q_1 ES - q_2 EI, \\ &\leq 1 - S - I. \\ \therefore \dot{V}_1 + V_1 &\leq 1 \Rightarrow \lim_{t \rightarrow \infty} V_1(t) \leq 1. \end{aligned}$$

So,

$$\lim_{t \rightarrow \infty} I(t) \leq 1.$$

Define a function $V_2 = \frac{1}{a}I(t - \tau) + \frac{1}{\alpha}P(t)$, taking its time derivative along the solution of the system (4), we have

$$\begin{aligned} \dot{V}_2 &\leq \beta S(t - \tau)I(t - \tau) - \frac{\mu}{a}I(t - \tau) - \frac{d}{\alpha}P(t), \\ &\leq \beta - \min\{\mu, d\}V_2. \\ \therefore \lim_{t \rightarrow \infty} P(t) &\leq M, \end{aligned}$$

where $M = \frac{\beta\alpha}{\min\{\mu, d\}}$. Hence, proposition follows.

References

1. Allee, W.C.: Animal Aggregations. A Study in General Sociology. University of Chicago Press, Chicago (1931)
2. Allen, J.C., Schaffer, W.M., Rosko, D.: Chaos reduces species extinctions by amplifying local population noise. *Nature* **364**, 229–232 (1993)
3. Angulo, E., Roemer, G.W., Berec, L., Gascoigen, J., Courchamp, F.: Double Allee effects and extinction in the island fox. *Conserv. Biol.* **21**, 1082–1091 (2007)
4. Bairagi, N., Roy, P.K., Chattopadhyay, J.: Role of infection on the stability of a predator–prey system with several response functions—a comparative study. *J. Theor. Biol.* **248**, 10–25 (2007)

5. Bairagi, N., Chaudhuri, S., Chattopadhyay, J.: Harvesting as a disease control measure in an eco-epidemiological system—a theoretical study. *Math. Biosci.* **217**, 134–144 (2009)
6. Berec, L., Angulo, E., Courchamp, F.: Multiple Allee effects and population management. *Trends Ecol. Evol.* **20**, 185–191 (2006)
7. Biswas, S., Sasmal, S.K., Samanta, S., Saifuddin, Md, Ahmed, Q.J.K., Chattopadhyay, J.: A delayed eco-epidemiological system with infected prey and predator subject to the weak Allee effect. *Math. Biosci.* **263**, 198–208 (2015)
8. Biswas, S., Sasmal, S.K., Saifuddin, Md, Chattopadhyay, J.: On existence of multiple periodic solutions for Lotka–Volterra’s predator–prey model with Allee effects. *Nonlinear Stud.* **22**(2), 189–199 (2015)
9. Biswas, S., Samanta, S., Chattopadhyay, J.: Cannibalistic predator–prey model with disease in predator—a delay model. *Int. J. Bifurc. Chaos* **25**(10), 1550130 (2015)
10. Biswas, S., Saifuddin, M., Sasmal, S.K., Samanta, S., Pal, N., Ababneh, F., Chattopadhyay, J.: A delayed prey–predator system with prey subject to the strong Allee effect and disease. *Nonlinear Dyn.* **84**, 1569–1594 (2016)
11. Chattopadhyay, J., Arino, O.: A predator–prey model with disease in the prey. *Nonlinear Anal.* **36**, 747–766 (1999)
12. Chattopadhyay, J., Bairagi, N.: Pelicans at risk in Salton Sea—an eco-epidemiological study. *Ecol. Model.* **136**, 103–112 (2001)
13. Chattopadhyay, J., Sarkar, R.R., Ghosal, G.: Removal of infected prey prevent limit cycle oscillations in an infected prey–predator system a mathematical study. *Ecol. Model.* **156**, 113–121 (2002)
14. Chaudhuri, K.S.: Dynamic optimization of combined harvesting of a two species fishery. *Ecol. Model.* **41**, 17–25 (1988)
15. Chen, Y., Yu, J., Sun, C.: Stability and Hopf bifurcation analysis in a three-level food chain system with delay. *Chaos Solitons Fract.* **31**, 683–694 (2007)
16. Clark, C.W.: *Bioeconomic Modelling and Fisheries Management*. Wiley, New York (1985)
17. Clark, C.W.: *Mathematical Bioeconomics: The Optimal Management of Renewable Resources*. Wiley, New York (1990)
18. Cohn, J.P.: Saving the Salton Sea. *Math. Biosci.* **50**(4), 295–301 (2000)
19. Courchamp, F., Clutton-Brock, T., Grenfell, B.: Multipack dynamics and the Allee effect in the African wild dog, *Lycaon pictus*. *Anim. Conserv.* **3**, 277–285 (2000)
20. Courchamp, F., Berec, L., Gascoigne, J.: *Allee Effects in Ecology and Conservation*. Oxford University Press, Oxford (2008)
21. Dong, T., Liao, X.: Bogdanov–Takens bifurcation in a trineuron BAM neural network model with multiple delays. *Nonlinear Dyn.* **71**(3), 583–595 (2013)
22. Drake, J.: Allee effects and the risk of biological invasion. *Risk Anal.* **24**, 795–802 (2004)
23. Gu, X., Zhu, W.: Stochastic optimal control of predator–prey ecosystem by using stochastic maximum principle. *Nonlinear Dyn.* 1–8 (2016)
24. Gulland, F.M.D.: *The Impact of Infectious Diseases on Wild Animal Populations—A Review, Ecology of Infectious Diseases in Natural Populations*. Cambridge University Press, Cambridge (1995)
25. Haderer, K.P., Freedman, H.I.: Predator–prey populations with parasitic infection. *J. Math. Biol.* **27**, 609–631 (1989)
26. Hale, J.K., Waltman, P.: Persistence in infinite-dimensional systems. *SIAM J. Math. Anal.* **20**(2), 388–395 (1989)
27. Hassard, B., Kazarinof, D., Wan, Y.: *Theory and Applications of Hopf Bifurcation*. Cambridge University Press, Cambridge (1981)
28. Hethcote, H.W., Wang, W., Han, L., Ma, Z.: A predator–prey model with infected prey. *Theor. Popul. Biol.* **66**, 259–268 (2004)
29. Hilker, F.M., Langlais, M., Petrovskii, S.V., Malchow, H.: A diffusive SI model with Allee effect and application to FIV. *Math. Biosci.* **206**, 61–80 (2007)
30. Huang, G., Takeuchi, Y.: Global analysis on delay epidemiological dynamic models with nonlinear incidence. *J. Math. Biol.* **63**(1), 125–139 (2011)
31. Huisman, J., Weissing, F.J.: Biodiversity of plankton by species oscillations and chaos. *Nature* **402**, 407–410 (1999)
32. Jana, S., Kar, T.: A mathematical study of a preypredator model in relevance to pest control. *Nonlinear Dyn.* **74**, 667–674 (2013)
33. Jana, S., Guria, S., Das, U., Kar, T., Ghorai, A.: Effect of harvesting and infection on predator in a prey–predator system. *Nonlinear Dyn.* **81**, 917–930 (2015)
34. Kang, Y., Sasmal, S.K., Bhowmick, A.R., Chattopadhyay, J.: Dynamics of a predator–prey system with prey subject to Allee effects and disease. *Math. Biosci. Eng.* **11**(4), 877–918 (2014)
35. Kuang, Y.: *Delay Differential Equation with Applications in Population Dynamics*. Academic Press, New York (1993)
36. Kumar, D., Chakrabarty, S.P.: A comparative study of bio-economic ratio-dependent predator–prey model with and without additional food to predator. *Nonlinear Dyn.* **80**(1–2), 23–38 (2015)
37. Lafferty, K.D., Morris, A.K.: Altered behaviour of parasitized killifish increases susceptibility to predation by bird final hosts. *Ecology* **77**, 1390–1397 (1996)
38. Leonel, R.J., Prunaret, D.F., Taha, A.K.: Big bang bifurcations and Allee effect in blumbergs dynamics. *Nonlinear Dyn.* **77**(4), 1749–1771 (2014)
39. Liao, M.X., Tang, X.H., Xu, C.J.: Bifurcation analysis for a three-species predator–prey system with two delays. *Commun. Nonlinear Sci. Numer. Simul.* **17**, 183–194 (2012)
40. Liu, Z., Yuan, R.: Stability and bifurcation in a delayed predator–prey system with Beddington–DeAngelis functional response. *J. Math. Anal. Appl.* **296**, 521–537 (2004)
41. Ma, J., Song, X., Jin, W., Wang, C.: Autapse-induced synchronization in a coupled neuronal network. *Chaos Solitons Fract.* **80**, 31–38 (2015)
42. Martin, A., Ruan, S.: Predator–prey models with delay and prey harvesting. *J. Math. Biol.* **43**(3), 247–267 (2001)
43. Meng, X.Y., Huo, H.F., Zhang, X.B., Xiang, H.: Stability and hopf bifurcation in a three-species system with feedback delays. *Nonlinear Dyn.* **64**, 349–364 (2011)
44. Mukandavire, Z., Garira, W., Chiyaka, C.: Asymptotic properties of an HIV/AIDS model with a time delay. *J. Math. Anal. Appl.* **330**(2), 916–933 (2007)

45. Myres, R., Barrowman, N., Hutchings, J., Rosenberg, A.: Population dynamics of exploited fish stocks at low population levels. *Science* **269**, 1106–1108 (1995)
46. Pablo, A.: A general class of predation models with multiplicative Allee effect. *Nonlinear Dyn.* **78**(1), 629–648 (2014)
47. Pal, N., Samanta, S., Biswas, S., Alquran, M., Al-Khaled, K., Chattopadhyay, J.: Stability and bifurcation analysis of a three-species food chain model with delay. *Int. J. Bifurc. Chaos* **25**(09), 1550123 (2015)
48. Peng, F., Kang, Y.: Dynamics of a modified lesliewooder model with double Allee effects. *Nonlinear Dyn.* **80**, 1051–1062 (2015)
49. Qin, H., Wu, Y., Wang, C., Ma, J.: Emitting waves from defects in network with autapses. *Commun. Nonlinear Sci. Numer. Simul.* **23**(1), 164–174 (2015)
50. Rohani, P., Miramontes, O., Hassell, M.: Quasiperiodicity and chaos in population models. *Proc. R. Soc. Lond. B: Biol. Sci.* **258**(1351), 17–22 (1994)
51. Saifuddin, M., Sasmal, S.K., Biswas, S., Sarkar, S., Alquran, M., Chattopadhyaya, J.: Effect of emergent carrying capacity in an eco-epidemiological system. *Math. Methods Appl. Sci.* **39**(4), 806–823 (2015)
52. Saifuddin, M., Biswas, S., Samanta, S., Sarkar, S., Chattopadhyaya, J.: Complex dynamics of an eco-epidemiological model with different competition coefficients and weak Allee in the predator. *Chaos Solitons Fract.* **91**, 270–285 (2016)
53. Sasmal, S.K., Chattopadhyay, J.: An eco-epidemiological system with infected prey and predator subject to the weak Allee effect. *Math. Biosci.* **246**, 260–271 (2013)
54. Sasmal, S.K., Bhowmick, A.R., Al-Khaled, K., Bhattacharya, S., Chattopadhyay, J.: Interplay of functional responses and weak Allee effect on pest control via viral infection or natural predator: an eco-epidemiological study. *Differ. Equ. Dyn. Syst.* **24**(1), 21–50 (2016)
55. Sasmal, S.K., Kang, Y., Chattopadhyay, J.: Intra-specific competition in predator can promote the coexistence of an eco-epidemiological model with strong Allee effects in prey. *BioSystems* **137**, 34–44 (2015)
56. Shi, J., Shivaji, R.: Persistence in reaction diffusion models with weak Allee effect. *J. Math. Biol.* **52**, 807–829 (2006)
57. Sun, C., Han, M., Lin, Y., Chen, Y.: Global qualitative analysis for a predator–prey system with delay. *Chaos Solitons Fract.* **32**(4), 1582–1596 (2007)
58. Taylor, C., Hastings, A.: Allee effects in biological invasions. *Ecol. Lett.* **8**, 895–908 (2005)
59. Wei, C., Chen, L.: Periodic solution and heteroclinic bifurcation in a predator–prey system with Allee effect and impulsive harvesting. *Nonlinear Dyn.* **76**(2), 1109–1117 (2014)
60. Wang, J., Jiang, W.: Bifurcation and chaos of a delayed predator–prey model with dormancy of predators. *Nonlinear Dyn.* **69**, 1541–1558 (2012)
61. Wolf, A., Swift, J., Swinney, H., Vastano, J.: Determining lyapunov exponents from a time series. *Phys. D* **16**, 285–317 (1985)
62. Xiao, Y., Chen, L.: Modelling and analysis of a predator–prey model with disease in the prey. *Math. Biosci.* **171**, 59–82 (2001)
63. Xu, C., Tang, X., Liao, M., He, X.: Bifurcation analysis in a delayed lotka–volterra predator–prey model with two delays. *Nonlinear Dyn.* **66**, 169–183 (2011)
64. Xua, R., Gan, Q., Ma, Z.: Stability and bifurcation analysis on a ratio-dependent predator–prey model with time delay. *J. Comput. Appl. Math.* **230**, 187–203 (2009)
65. Yan, J., Zhao, A., Yan, W.: Existence and global attractivity of periodic solution for an impulsive delay differential equation with Allee effect. *J. Math. Anal. Appl.* **309**, 489–504 (2005)
66. Yakubu, A.A.: Allee effects in a discrete-time SIS epidemic model with infected newborns. *J. Differ. Equ. Appl.* **13**, 341–356 (2007)
67. Yao, C., Ma, J., Li, C., He, Z.: The effect of process delay on dynamical behaviors in a self-feedback nonlinear oscillator. *Commun. Nonlinear Sci. Numer. Simul.* **39**, 99–107 (2016)
68. Zaman, G., Kang, Y.H., Jung, H.: Optimal treatment of an SIR epidemic model with time delay. *BioSystems* **98**, 43–50 (2009)
69. Zhou, S.R., Liu, Y.E., Wang, G.: The stability of predator–prey systems subject to the Allee effects. *Theor. Popul. Biol.* **67**, 23–31 (2005)